Chinese Chemical Letters 35 (2024) 108686

Contents lists available at ScienceDirect

Chinese Chemical Letters

journal homepage: www.elsevier.com/locate/cclet

Lidocaine hydrochloride loaded isomaltulose microneedles for efficient local anesthesia of the skin

Xuebing Jiang[a,1], Siyi Wang[a,b,1], Li Zhang[a], Xian Jiang[c], Maling Gou[a,*]

[a] State Key Laboratory of Biotherapy, West China Hospital, Sichuan University, Chengdu 610041, China
[b] Huahang Microcreate Technology Co., Ltd., Chengdu 610042, China
[c] Department of Dermatology, West China Hospital, Sichuan University, Chengdu 610041, China

ARTICLE INFO

Article history:
Received 10 April 2023
Revised 8 June 2023
Accepted 11 June 2023
Available online 16 June 2023

Keywords:
Microneedles
Local anesthesia
Lidocaine hydrochloride
Isomaltulose
Transdermal delivery

ABSTRACT

Lidocaine hydrochloride (LIDH) as an anesthetic is widely used in local anesthesia. Dissolving microneedles (MNs) have great application value in the field of skin anesthesia. However, the limited drug-loading of dissolving MNs is an existing challenge that affects clinical use. In this study, we have screened isomaltulose (ISO) as the proper matrix material for the MNs by using molecular dynamics (MD) simulation. Our findings indicate that ISO has good compatibility with LIDH, and the LIDH-loaded ISO MNs (LI-MNs) have high drug-loading capacity. The drug-loading capacity of LI-MNs could reach 80%, and it could effectively puncture the skin. In addition, the preparation method of customized LI-MNs was established based on three-dimensional (3D) printing technology. It was shown that the administration time of LI-MNs could be controlled within 3 min. Also, the LI-MNs were able to provide the local anesthetic efficacy within 2 min and sustained for more than 2 h. Significantly, LI-MNs had more efficient drug efficacy compared to the topical creams and the majority of existing LIDH-loaded dissolving MNs. They even provided a longer duration of action than the injections. Overall, the LI-MNs with high drug-loading have a promising application prospect.

Lidocaine hydrochloride (LIDH) is a local amide anesthetic and is widely used in clinical local anesthesia, such as dermatological procedures and biopsies [1]. With the widening use of minor surgical procedures, the demand of local anesthesia for the skin increases. The most common way of delivering local anesthesia to patients in clinical practice is to inject anesthetic drugs. However, the direct injection of drugs inherently caused pain. LIDH creams have been developed to reduce pain, but the slow-acting of the LIDH creams would restrict clinical applications [2–4]. The stratum corneum serves as the natural physical barrier to limit drug diffusion through the skin, which is the primary cause of it [5–7].

As a minimally invasive skin puncture device, dissolving microneedles (MNs) can penetrate the stratum corneum of the skin and create microchannels to facilitate the penetration of drug molecules into the dermis, resulting in local or systemic therapeutic effects [8–11]. The penetration depth of the dissolving MNs does not reach the nerve endings, so the pain can be effectively avoided [12]. The dissolving MNs are prepared by using a dissolvable matrix material loaded with drugs that do not leave any sharp waste in the body. In addition, as a disposable device, the dissolving MNs can reduce the possibility of drug cross-contamination which ensures patients' safety. The LIDH-loaded dissolving MNs have been studied for decades, but their restricted drug-loading capacity remains an issue. It may cause problems, such as slow onset or short duration of action [13,14]. Therefore, the application value of dissolving MNs as a dosage form is still constrained in local anesthesia.

In this study, we aim to work on a matrix material to achieve the preparation of the high drug-loading dissolving MNs, so that the MNs could deliver more doses of LIDH to the patients. The molecular dynamics (MD) simulations is an effective computer-aided tool that can be used to guide experimental study [15]. It has the advantages of fast calculation speed, small errors between simulation and experimental results, and low consumption of manpower and material resources [16]. We used MD simulations to find a proper matrix material. Subsequently, preparation methods based on 3D printing technology were used in this study, allowing for the quick customization of MNs. Further, the practical applicability of the MNs was verified by the skin puncture tests, drug delivery capability, and biosafety tests. Finally, the actual efficacy of MNs, including onset and duration of action, was examined

* Corresponding author.
E-mail address: goumaling@scu.edu.cn (M. Gou).
[1] These authors contributed equally to this work.

https://doi.org/10.1016/j.cclet.2023.108686
1001-8417/

Table 1
The interaction energy of hybrid systems (unit: kcal/mol).

Hybrid system	E_{total}	E_{LIDH}	E_{matrix}	E_{inter}
LIDH/ISO	566.30	287.11	309.31	−30.13
LDIH/MAL	575.72	287.11	309.78	−21.17
LIDH/PVA	−199.48	−23.62	−165.96	−9.91
LIDH/CTS	1279.79	−23.62	1299.82	3.59
LIDH/PVP	−25.87	−23.62	−26.71	24.45
LIDH/HPMC	175.10	−23.62	199.80	−1.07
LIDH/CMC	−268.44	−23.62	−262.66	17.84
LIDH/HA	−9.48	−23.62	−18.85	32.99
LIDH/SA	−200.92	−23.62	−227.02	49.73
LIDH/PLGA	141.08	−23.62	146.67	18.03
LIDH/PMVE/MA	−199.95	−23.62	−181.78	5.45

through behavioral experiments on animals. We also compared the efficacy of our MNs with that of the current existing topical creams and injections.

We selected eleven commonly used matrix materials to screen, including hyaluronic acid (HA), sodium hyaluronate (SA), carboxymethylcellulose (CMC), polyvinyl alcohol (PVA), polyvinylpyrrolidone (PVP), poly(methylvinyl ether)/(maleic anhydride) (PMVE/MA), hydroxypropyl methylcellulose (HPMC), poly(lactic-*co*-glycolic acid) (PLGA), chitosan (CTS), maltose (MAL), and isomaltulose (ISO). To screen a matrix material that had great compatibility with LIDH, the eleven hybrid systems were formed by mixing each of them with the LIDH. Then, we used Materials Studio 8.0 software to perform MD simulations in each of the hybrid systems and calculated the interaction energies [15,17,18]. The interaction energy (E_{inter}) could be used as a reference standard for evaluating the compatibility between different hybrid systems. When the total interaction energy became lower, the two substances would be more compatible and stable. As shown in Table 1, among the 11 matrix materials, the ISO had strong interactions with LIDH. The interaction energy of LIDH/ISO could reach −30.13 kcal/mol. It indicated that high drug-loading LIDH-loaded dissolving MNs could be prepared using ISO as the matrix material.

The LIDH-loaded ISO MNs (LI-MNs) were fabricated through three steps, consisting of the customized MNs master molds, the preparation of polydimethylsiloxane (PDMS) female molds, and the preparation of LI-MNs. The MNs master molds were customized by the static optical projection lithography (SOPL) technology [19]. It could help us get MNs master molds in seconds and quickly customize different shapes and sizes of MNs master molds to meet the needs of patients. Then, the PDMS female molds were prepared by using the membrane turning method on the basis of MNs master molds (Fig. 1A). The LI-MN contained the needle tips and the backing layer (Fig. S1 in Supporting information). The preparation of LI-MNs was described in detail below. First, the drug-melting mixtures were prepared by mixing LIDH and ISO with a mass ratio of 8:2 at high temperatures. Then these mixtures were infilled into the PDMS female molds under a vacuum at 145 °C and maintained for minutes. The excess drug-melting mixtures at the surface were scrapped off to complete the preparation of the needle tips. Subsequently, the melted ISO was infilled into the PDMS female molds under a vacuum at 145 °C and maintained for minutes to prepare for the backing layer. After cooling to room temperature, the LI-MNs were peeled off the mold (Fig. 1B). The needle tip was comprised of the drug-melting mixtures, and the backing layer was comprised of melted ISO. The content of LIDH in the LI-MNs with 10 × 10 array was 13.02 ± 0.40 mg.

The morphology of the LI-MNs was observed by the microscope and the scanning electron microscope (SEM) at 15 kV. As shown in Fig. 1C, the microscopic observation exhibited that the base diameter, average height, and tip diameter of the LI-MNs

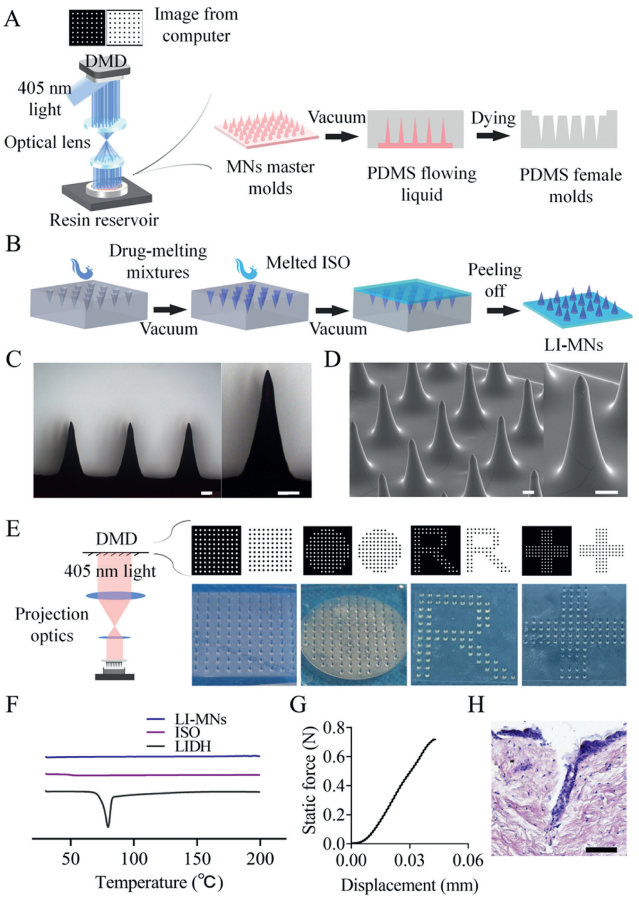

Fig. 1. Preparation and characterization of LI-MNs. The complete preparation process of LI-MNs included the preparation of MNs master molds, PDMS female molds (A), and the LI-MNs (B). (C) Overall appearance of LI-MN. Scale bar: 200 μm. (D) SEM image of LI-MN. Scale bar: 200 μm. (E) Customized LI-MNs photo. (F) DSC thermograms of LI-MNs, ISO, and LIDH. (G) Representative stress-displacement curve of one needle of the LI-MNs measured by the texture analyzer. (H) Histological examination of the skin section after the puncture with the LI-MNs. Scale bar: 100 μm.

were 420.40 ± 3.11 μm, 816.15 ± 6.17 μm, and 8.13 ± 0.35 μm, respectively. The area of the LI-MNs with 10 × 10 arrays was about 1.1 cm^2. The surface of the LI-MNs was smooth without any delaminations or particles (Fig. 1D) which could be attributed to the uniform dispersion of LIDH. Significantly, the shape of LI-MNs could be systematically controlled by our preparation method (Fig. 1E). To test whether the high temperature during the preparation method affected the drug stability, we dissolved the LI-MNs and the LIDH powder with the same drug content in distilled water (DW) and filtrated through a 0.22 μm microporous membrane filter respectively. Then, the filtrated solutions were analyzed by using high-performance liquid chromatography (HPLC). It was shown that the retention time of the LI-MNs was about 8.7 min, which was consistent with the solution of LDIH powder on the HPLC chromatogram (Fig. S2A in Supporting information). There was no significant difference in the content of LIDH between the LI-MNs and the LIDH powder (Fig. S2B in Supporting information). The result indicated that the efficacy of LIDH was not affected by the high temperature.

Further, the physical state of LIDH within the LI-MNs was studied by analyzing the differential scanning calorimetry (DSC) thermograms and X-ray diffraction (XRD) patterns. In Fig. 1F, the DSC thermograms of LIDH showed an endothermic drug peak at about 79 °C. The main reason for it was that LIDH was initially crystalline. However, the LI-MNs absented the endothermic drug peaks,

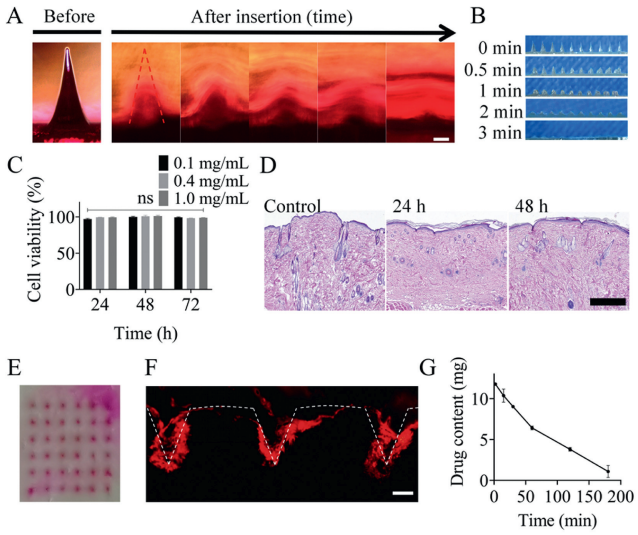

Fig. 2. Examination of the performance of LI-MNs. (A) The dissolution of LI-MNs in the agarose gel. Scale bar: 200 μm. (B) Representative images displaying the morphology of MNs' needle tips were taken out at different time intervals after penetrating the rat's skin. (C) The effects of 0.1, 0.4, and 1 mg/mL concentrations of extraction solutions on HSF cell viability that was evaluated with CCK-8 assay. The data were expressed as mean ± standard deviation (SD), $n = 3$. ns, no significance. (D) Histological examination of skin at 24 h and 48 h after the LI-MNs treatment and comparison with the skin before treatment. Scale bar: 500 μm. (E) Rat's skin was stained with rhodamine B after being punctured with LI-MNs. (F) Frozen sections showed that LI-MNs delivered rhodamine B to the rat's skin. Scale bar: 200 μm. (G) Line graph of the content of LIDH in the skin with time after being punctured with LI-MNs. The data were expressed as mean ± standard deviation (SD), $n = 3$.

which illustrated that LIDH was amorphous inside the ISO matrix. The main reason for it was that high temperature process destroys the original ordered crystal structure of LIDH. Compared to the XRD pattern of LIDH, the multiple peaks of the LI-MNs had disappeared which also revealed the transition of LIDH from crystalline to amorphous (Fig. S3 in Supporting information). Thus, the LIDH in LI-MNs was dispersed entirely and solubilized in the matrix materials. Fig. 1G demonstrated that the fracture force of LI-MNs was about 0.71 N/needle. The current study implied that the MNs could pierce the skin without being broken when the fracture force was above 0.24 N/needle [20]. It meant that the fracture force of the MNs was sufficient to pierce the skin. Moreover, a 0.1–3 N force was used to push the MNs into the skin [21,22]. The pushing force of the human thumb could reach at least 28.1 N [23], which was sufficient to insert the LI-MNs into the skin. Further, the skin puncture experiments were used to verify the actual puncturing effect of MNs. Animal welfare and experimental procedures were reviewed and approved by the Animal Ethics Committee of the State Key Laboratory of Biotherapy, Sichuan University. In our study, the LI-MNs were inserted into the rat's back skin. As shown in Fig. 1H, the insertion depth of the LI-MNs was about 318 μm, which revealed that the MNs pierced through the epidermis and reached the layer of the dermis. We also proved the skin insertion ability of LI-MNs by using pigskin because of its reality and similarity to human anatomy (Fig. S4 in Supporting information) [24].

Agarose gels could be used to observe the dissolution of the MNs [25]. To prepare the agarose gel with viscoelastic properties similar to the pigskin, we added agarose powder to the DW (0.0265 g/mL) [26], and the DW was heated to dissolve completely. Then, the solution stayed for 30 min at room temperature and molded into slices. To observe the dissolution of the MNs, we added rhodamine B (0.5% mass ratio) to the drug-melting mixtures to prepare the LI-MNs with rhodamine B. As shown in Fig. 2A, the MNs completely dissolved within 2 min. In addition, the diffusion of the MNs in agarose gel was uniform and rapid (Fig. S5 in Supporting information). Applying the MNs to the rat's skin could characterize the MNs' dissolution properties when we used them. The rat's back skin was divided into four parts, and each part was used with an LI-MN**.** Subsequently, the LI-MNs were removed from the skin after 0.5, 1, 2, and 3 min, respectively. As shown in Fig. 2B, it took 3 min for the LI-MNs to dissolve *in vivo*. The dissolution time of the LI-MNs *in vivo* was longer compared to the dissolution time *in vitro*. The possible reason could be that the moisture content of the agarose gel was higher than the skin's moisture content**.** The biosafety of the LI-MNs was further investigated, including the cytotoxicity assay and the inflammatory immune response *in vivo*. Cytotoxicity of the LI-MNs toward human skin fibroblast (HSF) was analyzed by cell counting kit-8 (CCK-8) assay. LI-MNs were dissolved in the culture medium to be configured into different concentrations of extraction solutions. As shown in Fig. 2C, the cell viability treated with extracts of 0.1–1.0 mg/mL concentrations persisted more than 95% within the 3 days, indicating that the materials had no adverse effect on the cells. Furthermore, the skin irritation of LI-MNs was tested by histological analysis. LI-MNs were used on rats, and the treated skins were collected after 24 h and 48 h. The skin that was not treated by LI-MNs worked as a control group. Then, these skin samples were fixed in 4% paraformaldehyde and were processed routinely into paraffin sections (5 μm). Compared to the untreated skin samples, the hematoxylin-eosin (H&E) staining results exhibited no apparent infiltrated inflammatory cells observed on the skin tissue on day 1 and day 2, indicating that the applications of LI-MNs did not harm the skin sample (Fig. 2D).

To observe the drug delivery capacity of the MNs, we pierced the LI-MNs with rhodamine B into the rat's back skin. The pinholes observed on the skin surface could be aligned with the array of the LI-MNs (Fig. 2E). Then, the skin was prepared into frozen sections to observe the drug delivery positions under a fluorescence microscope. As shown in Fig. 2F, the red fluorescence emitted by rhodamine B could be clearly observed at the pinholes. As a drug dosage form, the drug delivery capacity of LI-MNs had been proven. Furthermore, we measured the content of the LIDH in the skin samples at different time points after administration of the LI-MNs. As shown in Fig. 2G, the drug diffused in the rat's skin as time passed, and the intradermal drug content decreased. Approximately 3.45 mg/cm^2 LIDH was significantly present in the skin samples at 2 h. The previous studies suggested that 2 mg of LIDH delivered into 1 cm^2 of skin could provide a local anesthetic action [27]. Therefore, the drug release results revealed that LI-MNs could maintain a local anesthetic level for more than 2 h.

To assess the local anesthetic effect of the LI-MNs, we measured the pain thresholds of the rats by the Von Frey test. The Von Frey test verifies the pain threshold of animals under a free-ranging state, avoiding stress on the animal that could affect the results of the experiment. The mid-plantar surface just posterior to the footpads, shown as the black dotted square in Fig. 3A, was used for pain testing. It was primarily innervated by terminal branches of the sciatic nerve [28]. The rats were divided into 5 groups consisting of the LI-MNs, Sham (no treatment), the ISO-MNs (prepared in the same method as LI-MNs but without the addition of LIDH), the LIDH-CR (LIDH cream), and the LIDH-IN (LIDH injection (2%)) (Fig. 3B). Depending on the size of the drug delivery site, 6 × 6 arrays of LI-MNs and ISO-MNs were designed and used. The LI-MNs, LIDH-CR, and LIDH-IN maintained a consistent amount of LIDH administered (about 4.68 mg). The LI-MNs started to take effect after 2 min ($P < 0.01$) of administration and maintained for more than 120 min ($P < 0.05$). The ISO-MNs showed no anesthetic effect (Fig. 3C). Compared to the sham group, the onset time of LIDH-IH and LIDH-CR were 2 min ($P < 0.01$) and 30 min ($P < 0.05$) respec-

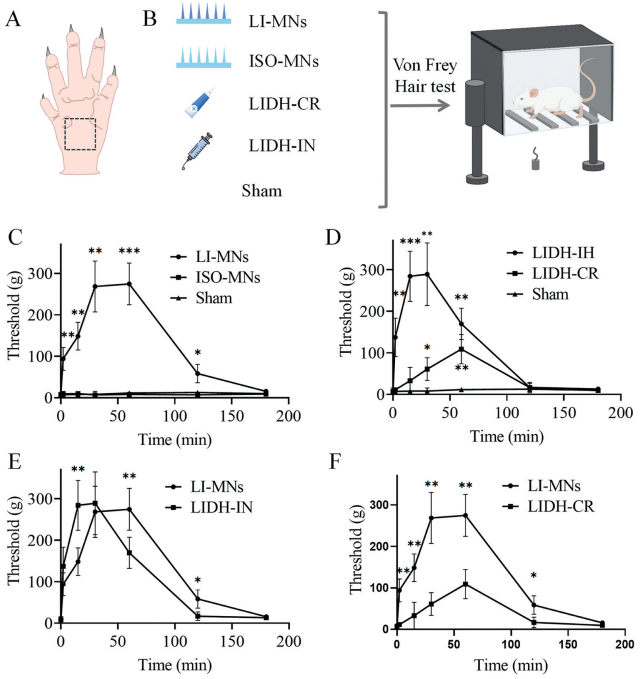

Fig. 3. Behavioral experiments on animals. (A) Diagram of the hindpaw area used for testing. (B) The schematic device of behavior test for measuring pain threshold. Anesthetic efficacy of LI-MNs, ISO-MNs (C), LIDH-IN, and LIDH-CR (D) compared with the Sham group. (E) Comparing the pain threshold according to time after LI-MNs and LIDH-IN application. (F) Comparing the pain threshold according to time after LI-MNs and LIDH-CR application. The data were expressed as mean ± SD, $n = 6$. $^{*}P < 0.05$, $^{**}P < 0.01$, $^{***}P < 0.001$.

tively, and the maintenance of the drug effect were all less than 120 min (Fig. 3D). When comparing the anesthetic effects of the LIDH-IN and LI-MNs, we found that the pain threshold of the injections was significantly higher than that of the MNs in the early stage but was generally lower than that of the MNs in the late stage. The drug effect of MNs was maintained longer than that of injections (Fig. 3E). The main reason for it might be that the vascular tissue under the skin was richer compared to the intracutaneous. When LIDH was injected into the subcutis, the drug was rapidly absorbed and utilized. However, the drug within the MNs was delivered to the superficial dermis, which meant that it required further release to be absorbed and utilized. Based on the above reasons, the drug delivered by injection was metabolized more quickly, while MNs could significantly prolong the duration of action. At the same time, we were concerned that it would show no significant difference in the pain thresholds between the LI-MNs and LIDH-IH at 30 min, indicating that the LI-MNs delivery approach could also provide a high pain tolerance similar to the LIDH-IH. As shown in Fig. 3F, the LI-MNs significantly improved the local anesthetic effect compared with the LIDH-CR. The main reason for this is that MNs can break the stratum corneum, whereas creams have a slow drug release rate due to the barrier of the skin. The results of the *in vitro* drug release showed a significant difference between the LI-MNs and LIDH-CR (Fig. S6 in Supporting information). About 93% of LIDH was released by LI-MNs at 4 h, but only 39% of LIDH was released by LIDH-CR at 12 h.

Combination of MD simulation and experimental techniques provides a priori means to solve biomedical problems [29]. We screened ISO as the matrix material by using MD simulation for the preparation of LI-MNs with high drug-loading. To ensure that the drug in the MNs could be used efficiently, we loaded LIDH only at the needle tips of the MNs. Each needle tip of LI-MNs could be loaded up with about 130.20 μg of LIDH which might be the highest drug-loading among the existing LIDH-loaded dissolving MNs [1,13,14,30]. The high drug-loading capacity made LI-MNs have the characteristics of both rapid onset and long duration of action. In addition, we could customize the LI-MNs to match the shape of the drug delivery site, which enhanced the practicality. The LI-MNs were biocompatible and do not cause inflammatory skin reactions. Also, the LI-MNs had universal applicability to patients due to the non-glycemic index of ISO. The previous study proved that topical applied LIDH was mainly distributed inside the skin [31]. Therefore, the *in vivo* drug release assay confirmed that the local skin still contained the drug content that could provide local anesthesia after 2 h of administration. The LI-MNs could be rapidly dissolved in the skin within 3 min and provided fast onset time and long duration of action. Animal behavioral experiments have declared that the local anesthetic effect of LI-MNs was better than that of topical creams. Compared with the injections, the LI-MNs had longer duration of action. In conclusion, the LI-MNs had efficient local anesthetic effects. Our study on the LI-MNs offers promising application prospects for the use of dissolving MNs in rapid local anesthesia of the skin.

Declaration of competing interest

The authors declare that they have no known competing financial interests or personal relationships that could have appeared to influence the work reported in this paper.

Acknowledgments

We thank Boya Li for the language help. We thank the Analytical and Testing Center, Sichuan University, for the provision of Materials Studio 8.0 software. We also thank H. Wang from the Analytical and Testing Center, Sichuan University, for the SEM observation and analysis of the data.

This work was supported by the National Key Research and Development Program of China (No. 2021YFF1200800), the Sichuan Science and Technology Program (Nos. 2021JDTD0001, 2022YFQ0004), and the Natural Science Foundation of Sichuan Province (No. 2023NSFSC1629).

Supplementary materials

Supplementary material associated with this article can be found, in the online version, at doi:10.1016/j.cclet.2023.108686.

References

[1] H. Yang, G. Kang, M. Jang, et al., Pharmaceutics 12 (2020) 1067.
[2] M. Horikiri, K. Ueda, T. Sakaba, J. Plast. Surg. Hand Surg. 52 (2018) 94–96.
[3] K. Kabashima, T. Honda, F. Ginhoux, G. Egawa, Nat. Rev. Immunol. 19 (2019) 19–30.
[4] M. Kumar, R. Chawla, M. Goyal, J. Anaesthesiol. Clin. Pharmacol. 31 (2015) 450–456.
[5] M. Ali, S. Namjoshi, H.E. Benson, Y. Mohammed, T. Kumeria, J. Control. Release 347 (2022) 561–589.
[6] Z. Zeng, G. Jiang, T. Liu, et al., Biodes. Manuf. 4 (2021) 902–911.
[7] P. Das, S. Manna, S. Roy, S.K. Nandi, P. Basak, Burns Trauma 11 (2023) tkac058.
[8] M.R. Prausnitz, J. Adv. Drug Deliv. Rev. 56 (2004) 581–587.
[9] M. Sheng, Y. Chen, H. Li, Y. Zhang, Z. Zhang, Burns Trauma 11 (2023) tkad009.
[10] Y. Wang, A.A. Sheng, X. Jiang, et al., Bio-Des. Manuf. 6 (2023) 255–267.
[11] Y. Liu, T. Huang, Z. Qian, W. Chen, Chin. Chem. Lett. 34 (2023) 108103.
[12] S. Mdanda, P. Ubanako, P.P.D. Kondiah, P. Kumar, Y.E. Choonara, Polymers 13 (2021) 2405.
[13] J. Yu, Y. Xia, H. Zhang, et al., J. Drug Deliv. Sci. Technol. 78 (2022) 103984.
[14] H. Zhan, F. Ma, Y. Huang, et al., Eur. J. Pharm. Sci. 121 (2018) 330–337.
[15] Y. Wang, Y. Guo, S. Qiang, et al., Front. Pharmacol. 12 (2021) 764351.
[16] W.L. Jorgensen, Science 303 (2004) 1813–1818.
[17] Q. Gao, C. Lu, X.W. Wang, et al., J. Mol. Model. 24 (2018) 95.
[18] T.K. Min, T.L. Yoon, T.L. Lim, Mater. Res. Express 5 (2018) 065054.
[19] X. Liu, R. Li, X. Yuan, et al., ACS Appl. Mater. Interfaces 13 (2021) 60522–60530.
[20] J. Cui, J. Huang, Y. Yan, et al., J. Colloid Interface Sci. 617 (2022) 718–729.

[21] S.P. Davis, B.J. Landis, Z.H. Adams, M.G. Allen, M.R. Prausnitz, J. Biomech. 37 (2004) 1155–1163.
[22] N. Roxhed, T.C. Gasser, P. Griss, G.A. Holzapfel, G. Stemme, J. Microelectromech. Syst. 16 (2007) 1429–1440.
[23] L. Peebles, B. Norris, Appl. Ergon. 34 (2003) 73–88.
[24] J. Cho, G.H. Kang, E.C. Kim, et al., Emerg. Med. J. 25 (2008) 732–734.
[25] X. Zhang, X. Fu, G. Chen, Y. Wang, Y. Zhao, Adv. Sci. 8 (2021) 202101210.
[26] D. Zhang, D.B. Das, C.D. Rielly, J. Pharm. Sci. 103 (2014) 613–627.
[27] A. Rzhevskiy, A. Popov, C. Pavlov, et al., PLoS One 17 (2022) e0261641.
[28] P.J. Austin, A. Wu, G. Moalem-Taylor, J. Vis. Exp. (2012) 3393.
[29] X. Wu, L.Y. Xu, E.M. Li, G. Dong, Chem. Biol. Drug Des. 99 (2022) 789–800.
[30] B.M. Lee, C. Lee, S.F. Lahiji, et al., Pharmaceutics 12 (2020) 366.
[31] H. Kathuria, H. Li, J. Pan, et al., Pharm. Res. 33 (2016) 2653–2667.